5A.8 CENTRIFUGING OF SCATTERERS IN TORNADOES

David C. Dowell[1], Joshua Wurman[2], and Louis J. Wicker[3]
[1] National Center for Atmospheric Research, Boulder, CO
[2] School of Meteorology, University of Oklahoma, Norman, OK
[3] National Severe Storms Laboratory, Norman, OK

1. INTRODUCTION

High-resolution radar observations of tornadoes typically indicate a minimum in reflectivity associated with the tornado (Fig. 1) (Fujita 1981; Wurman and Gill 2000; Bluestein and Pazmany 2000). A tube of relatively high reflectivity often surrounds the weak-echo region. Near the surface, the weak-echo region may be narrow or even absent. Aloft, the width of the weak-echo eye generally increases with height. In previous studies, the characteristics of the distribution of scatterers (precipitation, dust, and/or debris) have been attributed to centrifugal ejection of particles by the tornado (Kangieser 1954, Das 1983, Snow 1984).

Within a strong vortex such as a tornado, the air motion typically differs from the motion of large radar targets (precipitation, debris, etc.). Therefore, a wind synthesis based on the radial motion of the scatterers does not reveal the true wind velocity.

2. ONE-DIMENSIONAL MODEL

In this section, we describe a simple model of particle motion within a vortex. The prescribed airflow is steady and has the characteristics of a Rankine combined vortex:

$$u_a(r) = 0 \tag{1}$$

$$v_a(r) = \frac{Vr}{R},\ r \le R \qquad v_a(r) = \frac{VR}{r},\ r \ge R \tag{2}$$

where u_a is the radial velocity of the air, v_a is the tangential velocity of the air, r is the distance from the vortex center, R is the radius of the vortex core, and V is the tangential velocity at the edge of the core. This vortex model, in which $u_a(r) = 0$ and $\partial v_a / \partial z = 0$, is most applicable to that portion of a tornado above the surface layer (Snow 1984). Modification of the airflow by precipitation loading has been considered in previous studies (Das 1983, Davies-Jones 2000). Since we are not interested here in how the vortex forms, we consider instead a steady flow and model the response of the precipitation distribution to it. Although it is also an important issue, we will not consider radar sampling issues associated with differential weighting by the reflectivity distribution.

The following equations govern the horizontal motion and number concentration of particles within the vortex:

$$\frac{\partial u_p}{\partial t} + u_p \frac{\partial u_p}{\partial r} - \frac{v_p^2}{r} = F_{drag}^{(u)} = -\frac{g u_p^2}{w_t^2} \tag{3}$$

$$\frac{\partial v_p}{\partial t} + u_p \frac{\partial v_p}{\partial r} + \frac{u_p v_p}{r} = F_{drag}^{(v)} = \frac{g(v_a - v_p)^2}{w_t^2} \tag{4}$$

Corresponding author address: David C. Dowell, National Center for Atmospheric Research, Advanced Studies Program, P. O. Box 3000, Boulder, CO 80307-3000; ddowell@ucar.edu

$$\frac{\partial n}{\partial t} + \frac{1}{r}\frac{\partial}{\partial r}(n r u_p) = 0 \tag{5}$$

where u_p is the radial velocity of the particle, v_p is the tangential velocity of the particle, F_{drag} is the drag force (per unit mass) exerted on the particle by the air, g is the acceleration of gravity, w_t is the terminal fall velocity of the particle, and n is the number concentration of the particles. Although w_t appears in (3) and (4), we do not include the vertical motions of particles explicitly. We have scaled the horizontal drag terms by terminal fall velocity because values of w_t are readily available for a number of scatterer types. The alternative expressions of the horizontal drag forces in explicit terms involving the drag coefficient are not as compact. Since a scale analysis (not shown) indicates that the magnitude of the pressure gradient force is relatively small for large, dense particles (precipitation and/or debris), the pressure gradient term has been neglected in (3). Mixing in (3)-(5) is also neglected.

We initialize the model with particle velocity components (u_p and v_p) that match those of the air. Since we are interested in relative, rather than absolute, magnitudes of number concentration, we have chosen to initialize the model with a uniform dimensionless number concentration of n=1.

3. RESULTS

For both of the experiments, the radius (R) of the vortex core and the maximum tangential velocity (V) are 100 m and 50 m s^{-1}, respectively. We simulated the motions of scatterers with different characteristics: 1. w_t =5 m s^{-1} (representative of large raindrops) and 2. w_t =20 m s^{-1} (representative of debris and/or small hailstones). We describe the horizontal motion of the scatterers below. In the future, we plan to examine how scatterers are distributed vertically. Large debris will tend to fall out and reduce the contamination to the radar data.

The radial and tangential velocity profiles of the scatterers quickly approach asymptotic solutions (Fig. 2). The debris particles are ejected outward at higher speed than the raindrops. The maxima in both the radial and tangential components of motion of the scatterers occur just outside the vortex core. Since the debris does not spend as much time in the zone of large tangential wind speeds, the peak tangential velocities of the debris are smaller than those of the rain. Since the peak in tangential velocity of the air at the edge of the core may not be as sharp in more realistic vortices, the difference between the tangential velocities of the debris and rain may be less in other cases.

Centrifuging of particles in the model quickly produces a minimum in number concentration within the vortex core and a surrounding annulus of relatively high number concentration (Fig. 3). These characteristics of the scatterer distribution are consistent with reflectivity observations of tornadoes. The degree of accumulation of particles in the annulus, and the rate of expansion of the annulus, are greater for the debris than for the rain. In these particular simulations,

there is no balanced state for the number concentration; particles are constantly ejected away from the center of the vortex. To produce an annulus of constant radius in the simulation, it would be necessary to introduce convergence and/or vertical variation of the airflow into the model.

If one were to erroneously characterize the mean vortex airflow based on radar samples of scatterer motion, the flow would appear anomalously divergent. (The actual airflow in the simulation is divergence-free.) The radial component of motion of the scatterers is divergent (i.e., $\partial u_p / \partial r$ is positive) within and just outside the vortex core, and convergent (i.e., $\partial u_p / \partial r$ is negative) at larger radii (Fig. 2a).

Away from the center of the vortex, the primary balance of terms in (3) is

$$\frac{v_p^2}{r} \approx \frac{g u_p^2}{w_t^2}. \tag{6}$$

The estimated mean divergence (δ) of the scatterer velocity within a circle of radius r concentric with the vortex is thus

$$\delta = \frac{2u_p}{r} \approx \frac{2v_p}{r}\frac{w_t}{\sqrt{rg}} = \frac{\zeta w_t}{\sqrt{rg}} \tag{7}$$

where ζ is the estimate of the mean vertical vorticity from the observations. For the simulated vortex, the magnitudes of δ are quite large within the vortex core (~0.15 s^{-1} for rain and ~0.30 s^{-1} for debris). A synthesis of vertical velocity based on the scatterer motions, without correction, would contain very large errors.

4. CONCLUSIONS AND FUTURE WORK

If one had perfect point measurements of Doppler velocity and knew the characteristic fall velocity of the scatterers, one could apply a correction to the radar data to obtain more realistic estimates of the radial velocity of the air. Unfortunately, such information is not typically available with observational datasets. To better understand the observed vertical variations of reflectivity in tornadoes, we plan to examine this topic with a two-dimensional axisymmetric numerical model.

ACKNOWLEDGMENTS

Initial work was funded by National Science Foundation (NSF) grant ATM-9612674 (Howard Bluestein, principal investigator). The lead author is currently supported by the National Center for Atmospheric Research (NCAR). NCAR is sponsored by NSF. Herb Stein provided documentation of the Almena, KS tornado.

REFERENCES

Bluestein, H. B., and A. L. Pazmany, 2000: Observations of tornadoes and other convective phenomena with a mobile, 3-mm wavelength, Doppler radar: The spring 1999 field experiment. *Bull. Amer. Meteor. Soc.*, **81**, 2939-2951.

Das, P., 1983: Vorticity concentration in the subcloud layers of a rotating cloud. Unpublished manuscript, 78 pp. [Available from Department of Atmospheric Sciences, Texas A&M University, College Station, Texas, 77843-3150.]

Davies-Jones, R. P., 2000: Can the hook echo instigate tornadogenesis barotropically? *Preprints, 20th Conf. on Severe Local Storms*, Orlando, FL, Amer. Meteor. Soc., 269-272.

Fujita, T. T., 1981: Tornadoes and downbursts in the context of generalized planetary scales. *J. Atmos. Sci.*, **38**, 1511-1534.

Kangieser, P. C., 1954: A physical explanation of the hollow structure of waterspout tubes. *Mon. Wea. Rev.,* **82**, 147-152.

Snow, J. T., 1984: On the formation of particle sheaths in columnar vortices. *J. Atmos. Sci*., **41**, 2477-2491.

Wurman, J., and S. Gill, 2000: Finescale radar observations of the Dimmitt, Texas (2 June 1995), Tornado. *Mon. Wea. Rev*., **128**, 2135-2164.

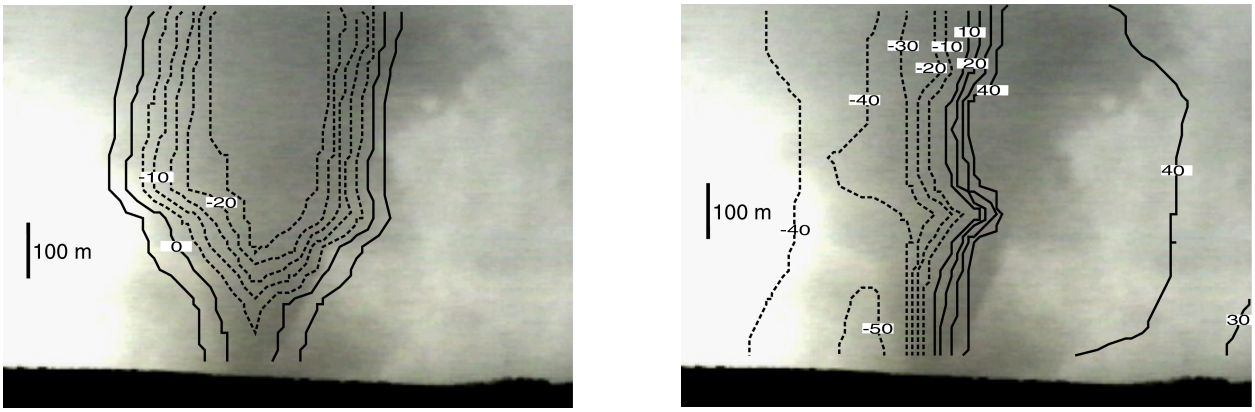

Figure 1. Vertical cross section of reflectivity factor (left, in dBZ_e, uncalibrated) and radial velocity (right, in m s^{-1}) from the Doppler on Wheels, superimposed onto an image (copyright 1999 by Herb Stein) of the Almena, KS tornado at 0037 UTC 4 June 1999. The grid spacing and radius of influence for the Cressman objective analysis of radar data were 50 m and 70 m, respectively.

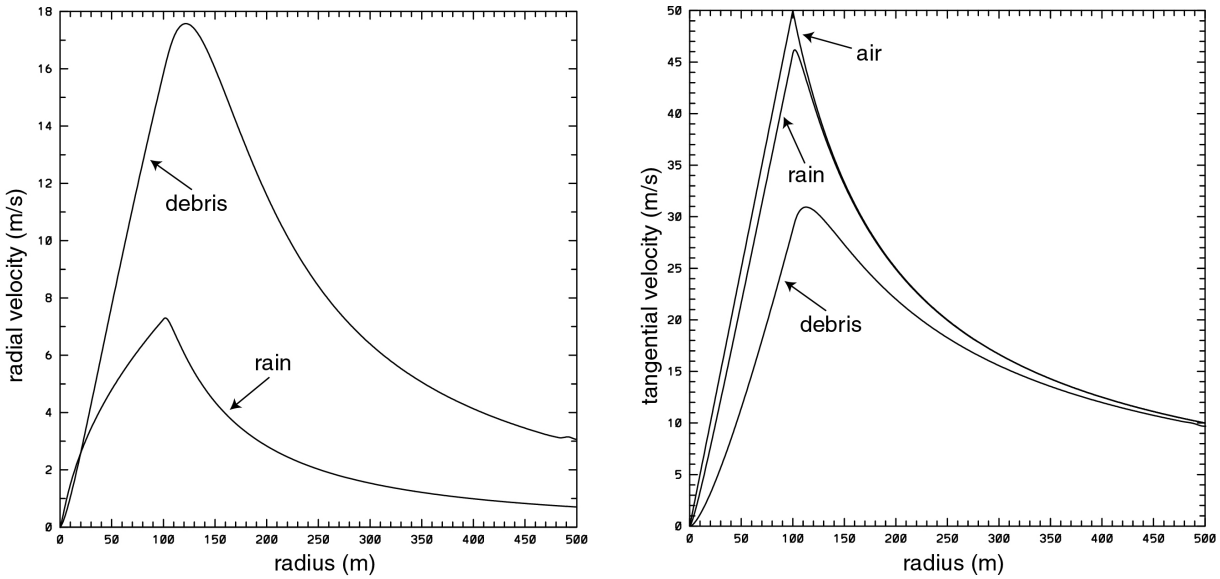

a) radial velocity component

b) tangential velocity component

Figure 2. Asymptotic solutions for the simulated scatterer motions, as a function of distance from the vortex core. The results apply to two classes of scatterers: large raindrops (w_t =5 m s^{-1}) and debris (w_t =20 m s^{-1}). The magnitude of the tangential velocity component of the air is also indicated.

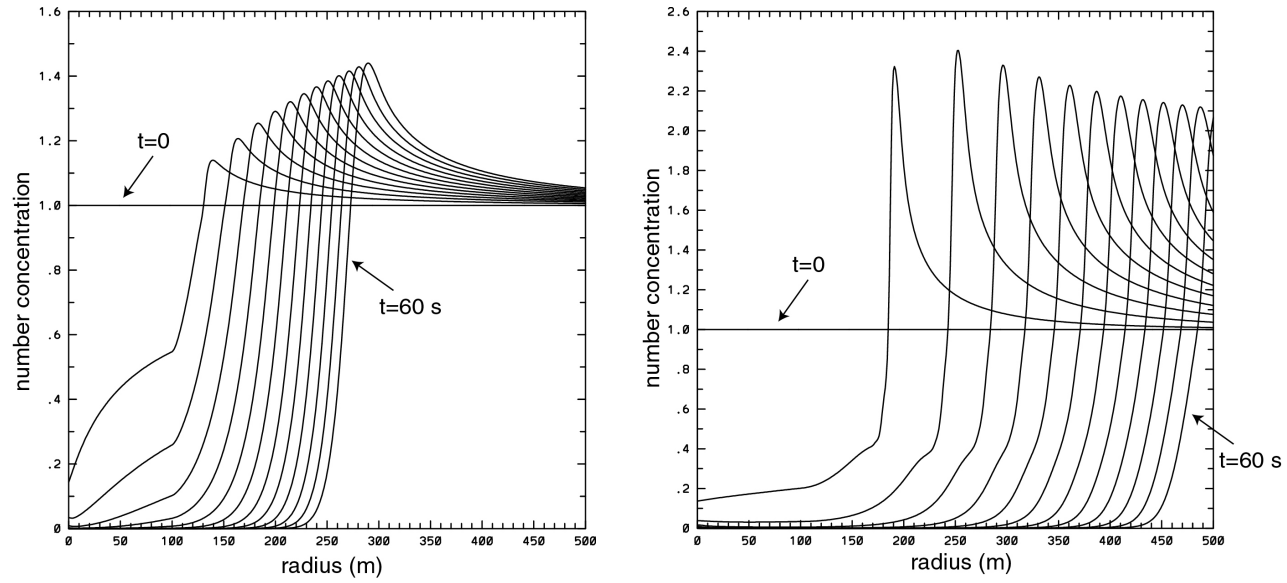

a) rain (w_t =5 m s^{-1})

b) debris (w_t =20 m s^{-1})

Figure 3. Scatterer number concentrations (dimensionless), as a function of time and distance from the vortex core. Results from the first 60 s of the simulations are shown at intervals of 5 s.